Catal Lett (2012) 142:22–31
DOI 10.1007/s10562-011-0727-7

Epoxidation of Propylene on a $[Ag_{14}O_9]$ Cluster Representing Ag_2O (001) Surface: A Density Functional Theory Study

Mehmet Ferdi Fellah · Isik Onal

Received: 12 September 2011 / Accepted: 18 October 2011 / Published online: 2 November 2011

Abstract Density functional theory calculations were employed to study partial oxidation of propylene on a $[Ag_{14}O_9]$ cluster representing Ag_2O (001) surface for which positive effect for ethylene oxide formation has been reported in our earlier work at the same level of theory (Fellah et al., Catal Lett 141:762, 2011). Propylene oxide (PO), propanal, acetone and Π-allyl radical formation reaction mechanisms were investigated. Π-allyl formation path and two propylene adsorption paths resulting in PO formation are competing reactions on silver oxide (001) surface because of their comparable activation barriers (9, 8 and 9 kcal/mol, respectively) while Π-allyl formation path is generally a more favorable path on Ag (111) surface as reported in previous theoretical literature. SO_2 adsorption calculations indicate that silver oxide has lower Lewis basicity relative to oxygen atom adsorbed on silver. Calculations also showed that surface oxygen atom of Ag_2O (001) has a higher spin density compared to that of oxygen atom adsorbed on Ag (111), which indicates that oxygen atom on Ag_2O (001) cluster has a more radical character.

Keywords DFT · Propylene epoxidation · Propylene oxide · Π-allyl · Silver oxide · Basicity

Present Address:
M. F. Fellah
Department of Chemical Engineering, Yuzuncu Yil University, Van 65080, Turkey

M. F. Fellah (✉) · I. Onal (✉)
Department of Chemical Engineering, Middle East Technical University, Ankara 06531, Turkey
e-mail: mffellah@gmail.com

I. Onal
e-mail: ional@metu.edu.tr

1 Introduction

Ethylene and propylene epoxides are versatile intermediates of great value to the chemical industry [1]. Ethylene oxide is produced on a very large scale by the direct silver-catalyzed heterogeneous partial oxidation of ethylene with oxygen. Considerable experimental effort has been devoted to understanding the mechanism of silver-catalyzed ethylene epoxidation as outlined in reviews [2–4]. The issues most often addressed have been the roles of oxygen and the promoters in the reaction. Grant and Lambert [5] carried out fundamental studies using primarily Ag (111) and Ag (110) single crystals which provided evidence for the key role of atomic rather than molecular oxygen in both the epoxidation and combustion reactions. Attempts to use the analogy of ethylene epoxidation in propylene epoxidation with molecular O_2 over Ag/Al_2O_3 catalyst, however, failed due to the presence of allylic H atoms in propylene, which upon facile abstraction result in rapid combustion of propylene to CO_2 and water. In a recent theoretical study it has been reported that PO selectivity has increased by a reaction between Π-allyl radical and propylene in gas phase [6]. Propene oxide (PO) is currently produced using two different types of commercial processes [1] (i) The chlorohydrin process which is environmentally unfriendly and (ii) The hydroperoxide process which produces large amounts of side products. As part of a continuing effort to understand the mechanism of olefin epoxidation, propylene oxidation on silver and copper (111) surfaces was investigated in a theoretical study [7]. They used VASP software and periodic method and reported that Π-allyl formation route was more favorable than propylene oxide formation route on silver surface. They studied aldehyde (propanal) formation route on both surfaces.

There is no theoretical study for propylene epoxidation on silver oxide in literature. Ethylene epoxidation was theoretically studied on surface oxide structures such as $Ag_{11}O_6$ [8–10] and $Ag_{12}O_6$ [10, 11] on silver (111) surface. Recent experimental and theoretical STM studies indicate formation of stoichiometries such as $Ag_{1.83}O$ [10] and $Ag_{1.33}O$ [12, 13]. Bocquet and co-workers [14, 15] have characterized two stable O phases which are low coverage (0.05 ± 0.02 ML) O adatom phase and an $Ag_{1.8}O$ oxide overlayer on Ag (111) by the scanning tunneling microscope (STM) and DFT. They reported that a DFT-derived phase diagram predicted that the $Ag_{1.8}O$ oxide overlayer would be stable under typical industrial conditions for epoxidation [15]. Bukhtiyarov et al. [16] reported that a stoichiometry of $Ag_{(x = 2 \pm 0.2)}O$ and an ionic component in the $Ag3d_{5/2}$ spectrum at 367.7 eV allow to conclude the formation of a surface silver (I) oxide which is confirmed by the similarity of its spectral characteristics with those of bulk Ag_2O. Recently Ag_2O (001) surface has been theoretically used for ethylene epoxidation in both cluster study [17] and periodic slab study [18]. These studies reported that silver oxide (001) surface has positive effect for ethylene oxide formation. Ethylene and propylene epoxidation reactions were also theoretically investigated on both Ag (111) and Ag_2O (001) surfaces [19]. Lu et al. [20] have reported in their experimental study that Ag_2O catalyst gave very low selectivity of propylene epoxide without further data.

The aim of this study is to investigate and compare propylene oxidation reaction pathways and to identify the mechanistic steps via which this reaction occurs on $Ag_{14}O_9$ surface cluster representing (001) surface by use of Density functional theory (DFT) calculations.

2 Surface Model and Calculation Method

All calculations in this study are based on DFT [21] as implemented in Gaussian'03 suite of programs [22]. In order to take into account the effects of exchange and correlation, Becke's [23, 24] three-parameter hybrid method involving the Lee, Yang, and Parr correlation functional (B3LYP) formalism [25] was used in this study. Los Alamos LANL2DZ effective core pseudo-potentials (ECP) for silver atoms and 6-31G(d,p) basis set for carbon, oxygen and hydrogen atoms were utilized. It has already been demonstrated [26] that hybrid B3LYP method is a high-quality density functional method certainly for this type of organic chemistry reactions. Silver oxide (Ag_2O) unit cell has a face centered cubic lattice structure with lattice parameter $a = 4.723$ Å and space group Pn-3 m and number 224 [27]. The silver oxide cluster was modeled as $Ag_{14}O_9$ cluster shown in Fig. 1. The cluster has the zigzag shape of OAgOAgO as the crystal oxide (001) surface which has same stoichiometry of Ag_2O catalyst. The active center atoms (Ag1, Ag2 and O1) have all of the neighboring atoms (Ag and O). The activation barrier data obtained for ethylene epoxidation by using the $Ag_{14}O_9$ (001) cluster [17] were in good agreement with those obtained on periodic silver oxide (001) slab surface [18]. Although it has been reported [28] that hydrogen termination does not prevent the strain effect on a cluster such as Pt_{35} cluster the dangling bonds of the silver and oxygen atoms were terminated with H atoms to obtain a neutral cluster. Terminating H atoms were not shown in the geometric representations. All of the cluster atoms except the active oxygen atom (O1) of the cluster were kept fixed. All of the atoms of the reactant and product molecules were relaxed. Energy profile and equilibrium geometry (EG) calculations were in general performed for determination of activation barriers and relative energies. Computed $<S^2>$ values confirmed that the spin contamination was very small (within max 0.9% after annihilation). Mulliken population analysis [29] was utilized to obtain Mulliken atomic charges. Natural bond orbital (NBO) [30] analysis has been used to obtain electronic configurations of metal atoms. Convergence criteria which are gradients of maximum force, root-mean-square (rms) force, maximum displacement, and rms displacement in Gaussian'03 software are 0.000450, 0.000300, 0.001800, and 0.001200, respectively.

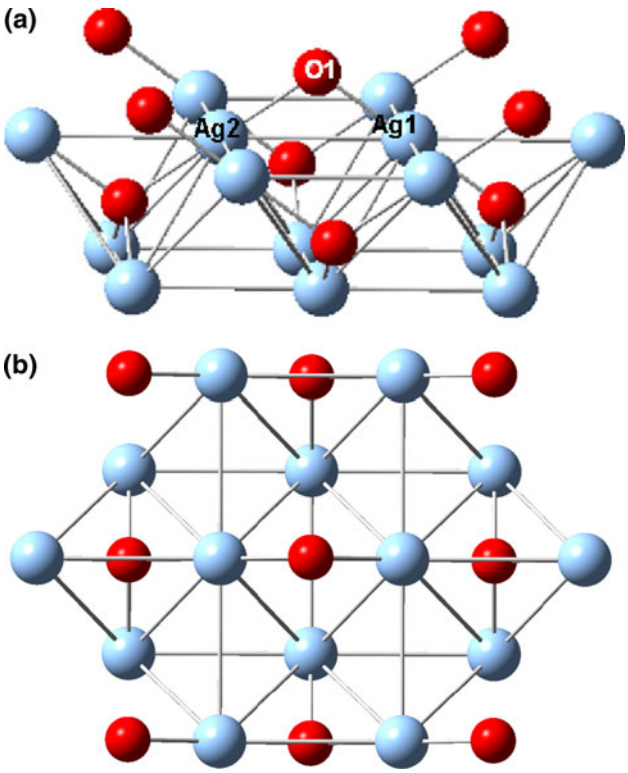

Fig. 1 $Ag_{14}O_9(001)$ surface cluster. **a** Side view. **b** Top view

The computational strategy employed in this study was as follows: Initially, the correct spin multiplicities for the cluster and adsorbing molecule were determined by Single Point Energy (SPE) calculations. SPE's were also calculated with different spin multiplicity numbers for each cluster-adsorbent system and the spin multiplicity number which corresponds to the lowest SPE was accepted as the correct spin multiplicity. The active oxygen atom (O1) of the cluster and the adsorbing molecule which is propylene were then fully optimized geometrically by means of EG calculations. The adsorbing molecule was first located over the active site of the cluster at a selected distance and a coordinate driving calculation was performed by selecting a reaction coordinate in order to obtain the variation of the relative energy with a decreasing reaction coordinate to get an energy profile as a function of the selected reaction coordinate distance. In the coordinate driving calculations all points on the reaction coordinate profile were optimized geometries. These energy profiles helped us to obtain transition state and final equilibrium geometries. The resulting relative energies for the cluster and reactant molecule complex are plotted against the reaction coordinate. The relative energy was defined as the following formula:

$$\Delta E = E_{System} - (E_{Cluster} + E_{Adsorbate})$$

where E_{System} is the calculated energy of the given geometry containing the cluster and the adsorbing molecule, $E_{Cluster}$ is the energy of the cluster, and $E_{Adsorbate}$ is that of the adsorbing molecule, e.g. propylene in this case. After obtaining the energy profile for the reaction step, the geometry with the minimum energy on the energy profile was then re-optimized by means of EG calculations to obtain the final geometry for the particular reaction step. Additionally, the geometry with the highest energy from the energy profile was taken as the input geometry for the transition state geometry calculations.

3 Results

Several products such as propylene oxide, propanal, acetone and Π-allyl radical can be formed during the partial oxidation of propylene with surface oxygen on the silver oxide cluster. Scheme 1 represents these possible paths. Following steps are the reactions for the oxidation of propylene on the cluster.

Step 1a: propylene adsorption—propyleneoxy formation (via first carbon)

$$[O_1]_{Ag_{14}O_9(001)Cluster} + C_3H_6 \rightarrow \left[C_{(O_1)}H_2CHCH_3\right]_{Ag_{14}O_9(001)Cluster} \quad (1)$$

Step 2a: propylene oxametallocycle (OMP1) formation

$$\left[C_{(O_1)}H_2CHCH_3\right]_{Ag_{14}O_9(001)Cluster} \rightarrow \left[C_{(O_1)}H_2C_{(Ag)}HCH_3\right]_{Ag_{14}O_9(001)Cluster} \quad (2)$$

Step 2b: propylene oxide formation

$$\left[C_{(O_1)}H_2CHCH_3\right]_{Ag_{14}O_9(001)Cluster} \rightarrow [C_3H_6O]_{Ag_{14}O_9(001)Cluster} \quad (3)$$

Step 1b: propylene adsorption—propyleneoxy formation (via second carbon)

$$[O_1]_{Ag_{14}O_9(001)Cluster} + C_3H_6 \rightarrow \left[CH_2C_{(O_1)}HCH_3\right]_{Ag_{14}O_9(001)Cluster} \quad (4)$$

Step 3a: propylene oxametallocycle (OMP2) formation

$$\left[CH_2C_{(O_1)}HCH_3\right]_{Ag_{14}O_9(001)Cluster} \rightarrow \left[C_{(Ag)}H_2C_{(O_1)}HCH_3\right]_{Ag_{14}O_9(001)Cluster} \quad (5)$$

Step 3b: propylene oxide formation

$$\left[CH_2C_{(O_1)}HCH_3\right]_{Ag_{14}O_9(001)Cluster} \rightarrow [C_3H_6O]_{Ag_{14}O_9(001)Cluster} \quad (6)$$

Step 2c: propanal formation

$$\left[C_{(O_1)}H_2CHCH_3\right]_{Ag_{14}O_9(001)Cluster} \rightarrow [CH_3CH_2CHO]_{Ag_{14}O_9(001)Cluster} \quad (7)$$

Step 3c: acetone formation

$$\left[CH_2C_{(O_1)}HCH_3\right]_{Ag_{14}O_9(001)Cluster} \rightarrow [CH_3COCH_3]_{Ag_{14}O_9(001)Cluster} \quad (8)$$

Step 1c: propylene adsorption—Π-allyl radical formation

$$[O_1]_{Ag_{14}O_9(001)Cluster} + C_3H_6 \rightarrow \left[H_{(O_1)}\right]_{Ag_{14}O_9(001)Cluster} + C_3H_5\bullet \quad (9)$$

Step 4: desorption of the products formed on the cluster

$$\left[(C_3H_6O) \text{ or } (CH_3CH_2CHO) \text{ or } (CH_3COCH_3)\right]_{Ag_{14}O_9(001)Cluster} \rightarrow [\,]_{Ag_{14}O_9(001)Cluster} + (C_3H_6O) \text{ or } (CH_3CH_2CHO) \text{ or } (CH_3COCH_3). \quad (10)$$

First step is the adsorption of propylene onto the oxygen atom of Ag_2O cluster. There are two reactions for adsorption of propylene on Ag_2O cluster. These reactions (steps 1a and b) resulted in surface intermediate, propylenoxy, formation have lower energy barriers (8 and 9 kcal/mol, respectively). Figures 2 and 3 show related geometries for steps 1a and b. As can be seen these figures, the final geometries were not similar to oxometallocycle molecules (OMP). The energies for the reaction of oxometallocycle intermediate formation (steps 2a and 3a)

Scheme 1 Possible reaction paths for partial oxidation of propylene

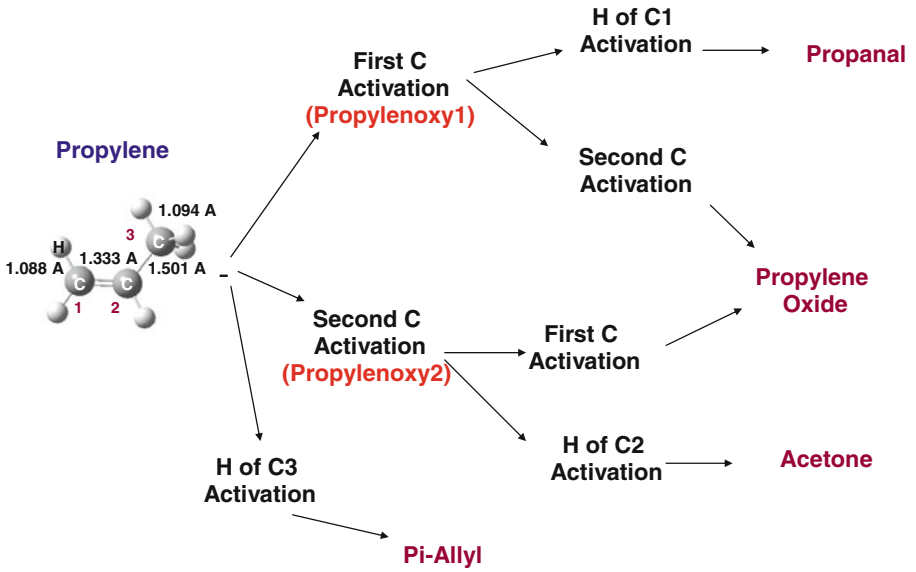

have increased exponentially, which means that oxometallocycle molecules were not formed on the silver oxide (001) surface. Next reactions (steps 2b and 3b) which are other possible reactions after the steps 1a and b, respectively are the formations of PO. The related geometries for these steps are represented in Figs. 4 and 5, respectively. Relative activation barriers for these reactions (steps 2b and 3b) were calculated to be 17 and 20 kcal/mol, respectively.

After the first and second carbon activation reactions (step 1a and b, propylenoxy formations), propanal and acetone molecules can be formed by activation of hydrogen atoms of first and second carbon atoms (steps 2c and 3c, respectively). Figures 6 and 7 depict the linked geometries obtained for these steps. Relative activation barriers for these reactions (steps 2c and 3c) were calculated to be 42 and 39 kcal/mol, respectively. Finally the last reaction (step 4) is desorption of products formed on the cluster.

A relative energy barrier of the reaction (step 1c, another alternative path for propylene adsorption) which gives Π-allyl radical is found as 9 kcal/mol when a reaction coordinate between the O1 atom of the cluster and one hydrogen atom of propylene molecule (H–O) was chosen. The energy profile for this reaction (step 1c) is shown in Fig. 8 to illustrate the methodology in obtaining relative energy profiles. The electronic properties of the silver centers in the respective structures are very similar (Table 1).

4 Discussion

A silver oxide (001) surface cluster including 14 silver atoms was used to propylene oxidation reactions. Table 1 shows Mulliken atomic charge and electronic configurations of Ag1, Ag2 and O1 atoms for equilibrium geometries for all

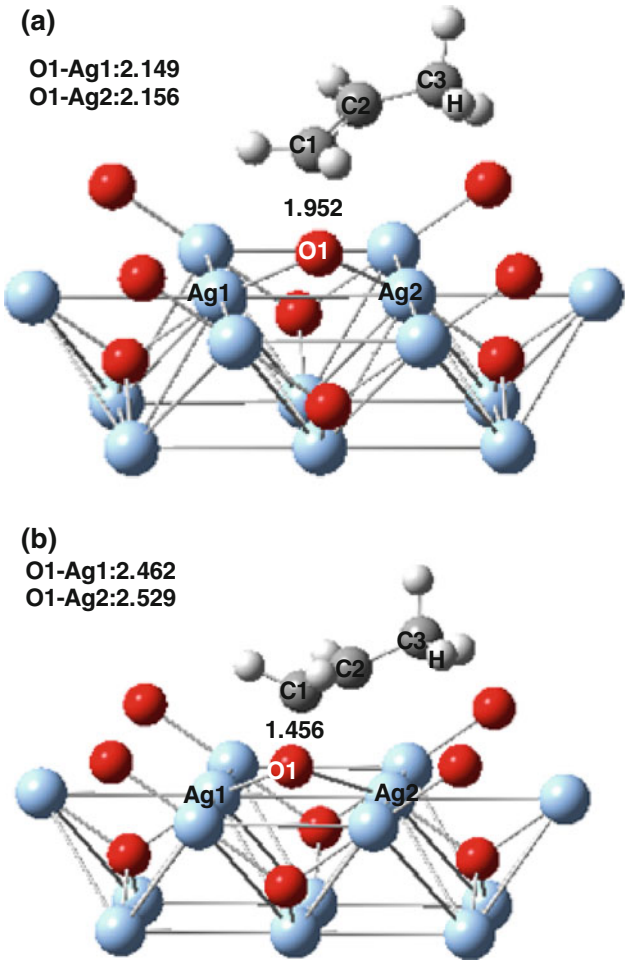

Fig. 2 **a** ATS geometry, **b** EG for propylene adsorption—propylenoxy formation (via first carbon) (step 1a) (Distance values in units of angstroms)

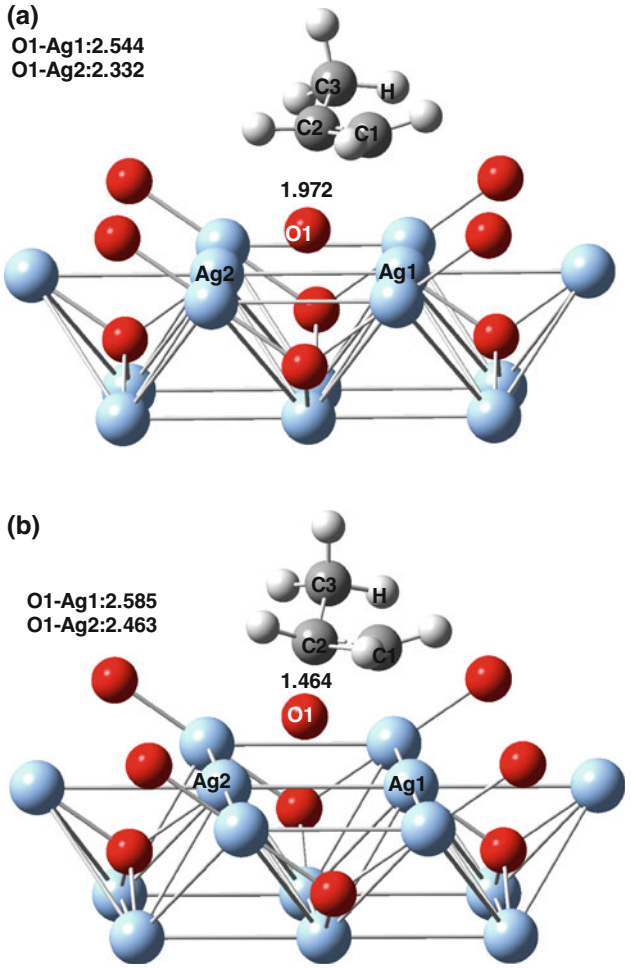

Fig. 3 **a** ATS geometry, **b** EG for propylene adsorption—propylenoxy formation (via second carbon) (step 1b) (Distance values in units of angstroms)

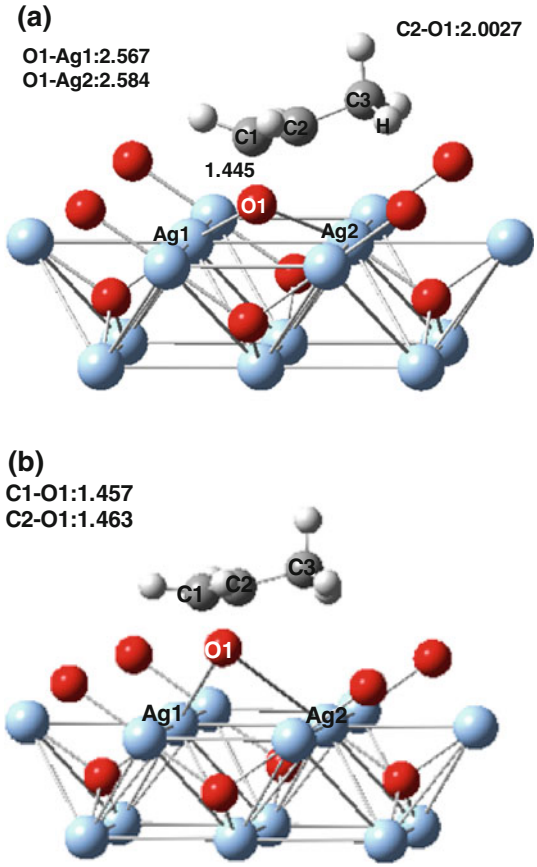

Fig. 4 **a** ATS geometry, **b** EG for propylene oxide formation (step 2b) (Distance values in units of angstroms)

reactions and cluster. The spin multiplicity number of the cluster was found as 7 by means of SPE calculations taking the total charge as neutral. However, after desorption of the products formed on the cluster, SM number of the cluster might be changed since the cluster has an oxygen vacancy. As seen from the Table 1, the atomic charge values of silver atoms (Ag1 and Ag2) on the cluster with oxygen vacancy are higher than those of the initial cluster, which shows more positive character on silver atoms in the cluster having a vacancy. It has already been reported that spin multiplicity number decreases with increasing atomic charge of active center metal [31] where different Fe-ZSM-5 clusters have been investigated for CO and NO adsorptions. In the same way, the SM of the cluster with oxygen vacancy was calculated to be 3 corresponding to lowest SPE. Thus, the SM number of 3 was used for the calculations to obtain desorption barriers of the products. Moreover, charge of oxygen (O1) atom on silver oxide surface was calculated to be −0.6. This matches well with the value of −0.7 computed on periodic slab surface of silver oxide [18].

All activation barriers were reported as the barrier based on coordinate driving calculations in this study. Their related geometries were also peak points corresponding to the highest energy of the relative energy profile where all points were optimized geometries. These approximate transition state (ATS) geometries were obtained along a reaction coordinate. According to our very recent theoretical experience [32–37], transition states geometries were very close to the peak points of the profiles. Moreover, the activation barriers based on ATS calculated for ethylene epoxidation by using the $Ag_{14}O_9$ (001) cluster [17] were in good agreement with the values computed on periodic silver oxide (001) slab surface [18].

Several products such as propylene oxide, propanal, acetone and Π-allyl radical can be formed during the oxidation of propylene with active oxygen on the cluster. These paths are shown in Scheme 1. Table 2 represents a comparison of activation barriers for partial oxidation reactions of propylene on both silver oxide (001) surface and silver (111) surface. Figure 9 also summarizes the relative energy diagram of reaction steps for the oxidation of propylene on silver oxide (001) cluster. As mentioned before, there are no activation barrier data in experimental

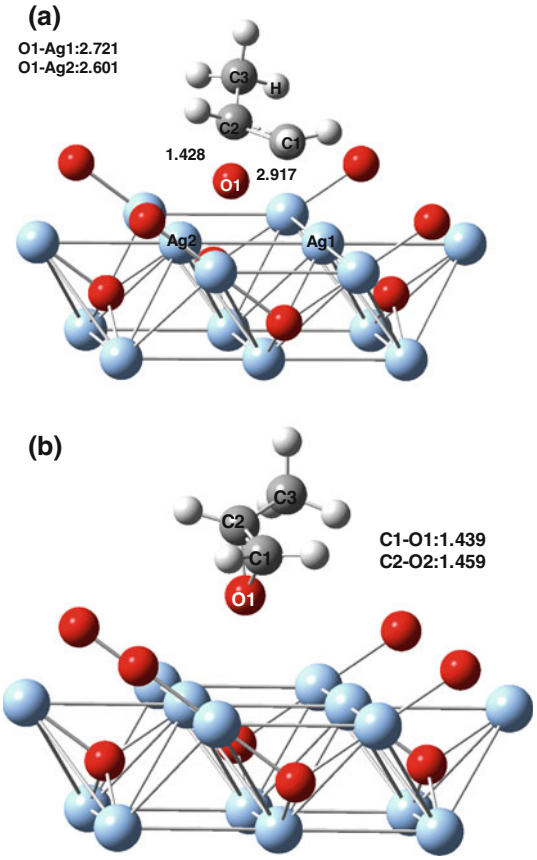

Fig. 5 **a** ATS geometry, **b** EG for propylene oxide formation (step 3b) (Distance values in units of angstroms)

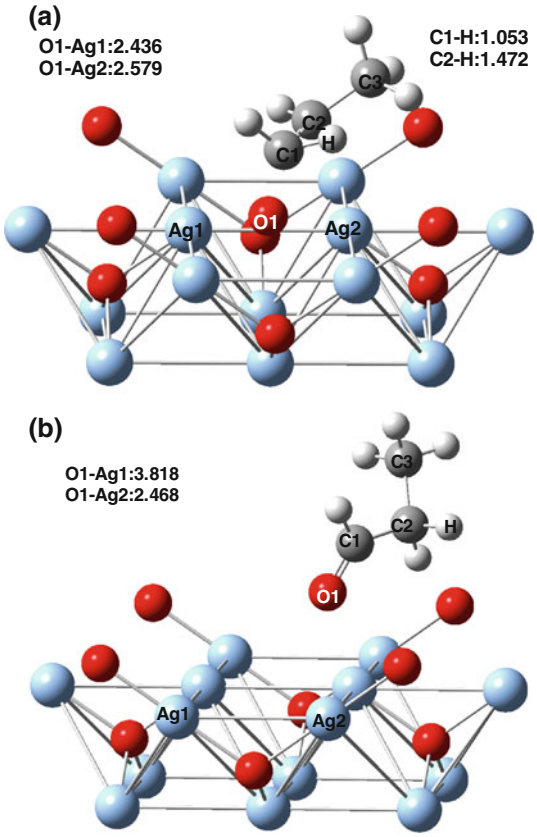

Fig. 6 **a** ATS geometry, **b** EG for propanal formation (step 2c) (Distance values in units of angstroms)

and theoretical literature for the possible reactions of propylene on silver oxide catalyst.

Activation barrier values for competing reactions of propylene adsorption (via C1 or C2 activation) which resulted in propylenoxy (surface intermediate) are calculated to be 8 and 9 kcal/mol, respectively. The activation energy barrier for the abstraction of allylic hydrogen atom of propylene by the oxygen atom of the cluster to form Π-allyl radical (step 1c) is found as 9 kcal/mol. In other words propylene adsorption reactions leading to PO formation competes with the Π-allyl formation reaction although it has been experimentally reported that Ag_2O catalyst gave very low selectivity of propylene epoxide without any further data [20]. Propylene oxametallocycles known as OMP are not formed at the end of the propylene adsorption reaction on silver oxide surface while these were formed on Ag (111) surface [7, 19]. Energy exponentially increased if reaction occurs to obtain OMP structure on the silver oxide surface (steps 2a and 3a). The activation barriers for propylene adsorption were reported as 14 kcal/mol [7] and 14 and 7 kcal/mol [19] on Ag (111) surface while it was reported as 7 [7] and 6 kcal/mol [19] for pi-allyl formation reaction. Propylene oxide formation reactions (via activation of C2 and C1, steps 2b and 3b, respectively) have activation barrier values of 17 and 20 kcal/mol, respectively. Torres et al. [7] have theoretically reported the activation barrier for propylene oxide formation via C2 activation was 14 kcal/mol on Ag (111) surface. Activation barrier values for propylene oxide formation paths on Ag (111) surface (via activation of C2 and C1) have been also reported [19] as 16 and 22 kcal/mol, respectively. Acetone and propanal formation reactions (steps 2c and 3c) have relatively higher activation barrier values (39 and 42 kcal/mol, respectively).

Pi-allyl formation path which is the undesired reaction for PO formation and propylene adsorption paths which result in the production of PO are competing with each other because of their comparable activation barriers (9 kcal/mol for Π-allyl formation and 8 and 9 kcal/mol for propylene adsorption reactions). On the other hand, Π-allyl molecule was easily formed on Ag (111) surface while propylene adsorption reaction had a higher activation barrier [7, 19]. Activation barriers of these reactions (Π-allyl formation and propylene adsorption paths) on Ag (111) surface were theoretically reported as 7 and 14 kcal/mol [7] and 6 and 14 kcal/mol [19]. Another most important difference between silver oxide surface used in this study

and silver surface [7, 19] is the formation of propylene oxametallocycles on those surfaces. These intermediate molecules are not formed on Ag_2O (001) surface while they are formed on silver (111) surface [7, 19]. The reason of this may be that silver oxide structure has sub-surface-oxygen atoms. The activation barriers for acetone and propanal formations are higher than those of propylene oxide formation paths. These barriers show that acetone and propanal have very low probabilities to be formed on Ag_2O surface while propylene oxide can be more easily formed on cluster. As can be seen from Table 2, activation barrier of propanal formation path especially increased on silver oxide surface as compared to that on silver surface.

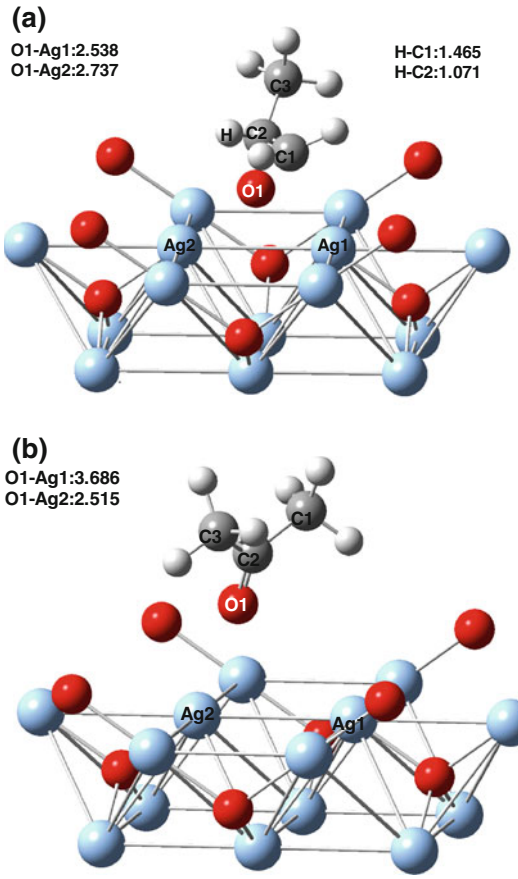

Fig. 7 **a** ATS geometry, **b** EG for acetone formation (step 3c) (Distance values in units of angstroms)

The selectivity values of the products for propylenoxy formation paths (given in steps 1a and b) which lead to either propylene oxide, propanal or acetone) and pi-allyl radical formation path (step 1c) are assumed to be 33.3, 33.3 and 33.3% respectively, based on their comparable activation barriers. In other words, the rate of pi-allyl radical formation path is equal to those of propylenoxy formation paths. Moreover, the total selectivity of propylene oxide can be accepted as 66.6% since activation barrier values of propanal and acetone formation paths (steps 2c and 3c) are substantially higher than those of PO formation paths (steps 2b and 3b), which take place after propylenoxy formations. As a result, one can conclude that pi-allyl formation path, which leads to combustion products, has relatively lower reaction rate with respect to those of PO formation paths.

A non-activated path which was reported for ethylene oxide formation on silver oxide surface [17, 18] is not observed for propylene epoxidation.

As mentioned before, PO formation paths compete with the Π-allyl formation path on silver oxide because of their comparable activation barriers. The reason of this may be that silver oxide structure has sub-surface-oxygen atoms.

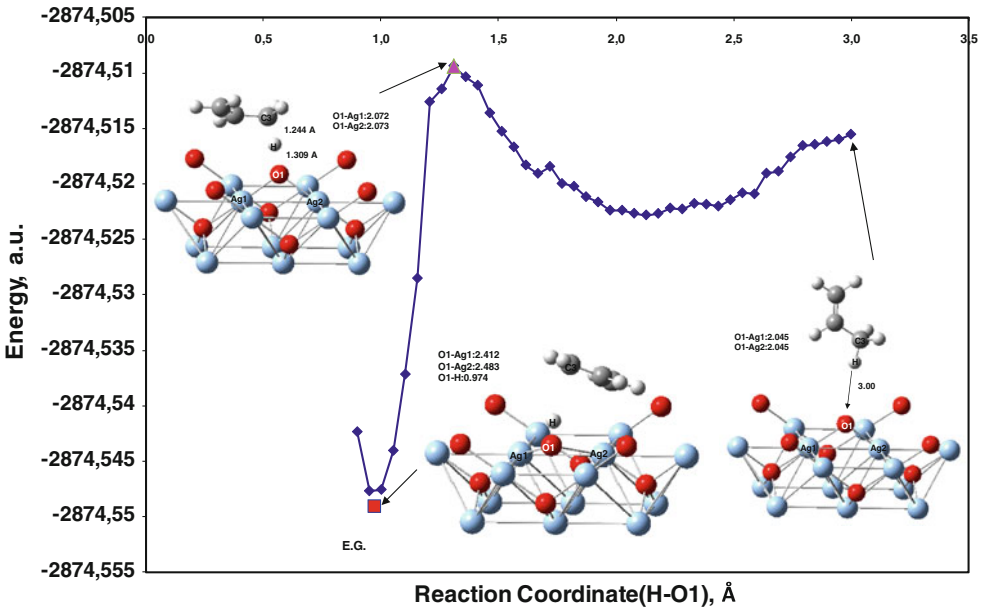

Fig. 8 Energy profile along reaction coordinate (H–O1) for Π-allyl formation path (step 1c) on (001) silver oxide surface cluster (Distance values in units of angstroms)

Table 1 Mulliken atomic charge values and electronic configurations of Ag1, Ag2 and O1 atoms for equilibrium geometries for all reactions and cluster

Reactions	Mulliken atomic charges			Electronic configurations	
	Ag1	Ag2	O1		
Cluster	+0.9	+1.0	−0.6	Ag1	[core]$5s^{0.31}4d^{4.83}5p^{0.02}6p^{0.01}$
				Ag2	[core]$5s^{0.31}4d^{4.84}5p^{0.02}6p^{0.01}$
				O1	[core]$2s^{1.93}2p^{5.03}$
Cluster with oxygen vacancy	+1.0	+1.1	–	Ag1	[core]$5s^{0.65}4d^{9.90}5p^{0.06}6s^{0.02}6p^{0.02}$
				Ag2	[core]$5s^{0.66}4d^{9.90}5p^{0.06}6s^{0.02}6p^{0.02}$
				O1	–
Propylene adsorption (first C activation, propylenoxy1, step 1a)	+12	+1.2	−0.6	Ag1	[core]$5s^{0.49}4d^{9.88}5p^{0.04}6s^{0.04}6p^{0.02}$
				Ag2	[core]$5s^{0.58}4d^{9.86}5p^{0.04}6s^{0.04}6p^{0.02}$
				O1	[core]$2s^{1.78}2p^{5.18}$
Propylene adsorption (second C activation, propylenoxy2, step 1b)	+1.1	+1.2	−0.6	Ag1	[core]$5s^{0.58}4d^{9.86}5p^{0.04}6s^{0.03}6p^{0.02}$
				Ag2	[core]$5s^{0.49}4d^{9.88}5p^{0.04}6s^{0.04}6p^{0.02}$
				O1	[core]$2s^{1.78}2p^{5.16}$
Propylene adsorption (Π-allyl formation, step 1c)	+1.4	+1.1	−0.7	Ag1	[core]$5s^{0.49}4d^{9.88}5p^{0.04}6s^{0.03}6p^{0.01}$
				Ag2	[core]$5s^{0.52}4d^{9.87}5p^{0.04}6s^{0.05}6p^{0.02}$
				O1	[core]$2s^{1.83}2p^{5.36}$
Propylene oxide formation (following C1 activation, step 2b)	+1.1	+1.1	−0.5	Ag1	[core]$5s^{0.70}4d^{9.90}5p^{0.05}6s^{0.02}6p^{0.02}$
				Ag2	[core]$5s^{0.72}4d^{9.90}5p^{0.05}6s^{0.02}6p^{0.02}$
				O1	[core]$2s^{1.72}2p^{4.90}3p^{0.01}3d^{0.01}$
Propylene oxide formation (following C2 activation, step 3b)	+1.2	+1.1	−0.5	Ag1	[core]$5s^{0.69}4d^{9.90}5p^{0.06}6s^{0.02}6p^{0.02}$
				Ag2	[core]$5s^{0.68}4d^{9.90}5p^{0.06}6s^{0.02}6p^{0.02}$
				O1	[core]$2s^{1.71}2p^{4.91}3p^{0.01}3d^{0.01}$
Propanal formation (step 2c)	+1.1	+1.2	−0.4	Ag1	[core]$5s^{0.62}4d^{9.91}5p^{0.05}6s^{0.02}6p^{0.02}$
				Ag2	[core]$5s^{0.60}4d^{9.89}5p^{0.05}6s^{0.03}6p^{0.02}$
				O1	[core]$2s^{1.70}2p^{4.89}3p^{0.01}3d^{0.01}$
Acetone formation (step 3c)	+1.3	+1.2	−0.4	Ag1	[core]$5s^{0.67}4d^{9.91}5p^{0.05}6s^{0.02}6p^{0.02}$
				Ag2	[core]$5s^{0.59}4d^{9.89}5p^{0.05}6s^{0.03}6p^{0.02}$
				O1	[core]$2s^{1.68}2p^{4.93}3p^{0.01}3d^{0.01}$

These sub-surface oxygen atoms might affect the activity of the surface oxygen atom on silver oxide. This effect might change the basicity of surface oxygen atom. Accordingly, we compared adsorption of SO_2 as a Lewis acid on both adsorbed oxygen atom on silver (111) and active oxygen atom on silver oxide (001) surfaces [17]. The binding energies of SO_2 to O atom on silver and silver oxide surfaces were computed as 53 and 34 kcal/mol, respectively. The value calculated for the oxygen atom on silver (111) is in reasonable agreement with the value of 57 kcal/mol obtained on periodic silver (111) slab surface by Torres et al. [7]. As a conclusion based on basicity calculations, the essential reason for not obtaining oxometallocycle as an intermediate molecule on silver oxide and competing of PO and Π-allyl formation paths is lower basicity of surface oxygen atom of silver oxide compared to O atom on Ag (111) surface. Moreover, the reason of these might be explained by that surface active oxygen atom (O1) of silver oxide (001) surface has higher spin density value (0.405) than the value of 0.320 of oxygen atom on Ag (111) surface. This shows that oxygen atom on Ag_2O (001) cluster has more radical character. The oxygen atoms with spin densities (radical character) over atomic clusters have been studied experimentally and theoretically [38–40].

5 Conclusions

Propylene partial oxidation reaction steps were investigated by using DFT calculations on a $[Ag_{14}O_9]$ cluster model representing silver oxide (001) surface. Theoretical computations on silver oxide surface showed that Π-allyl formation path and propylene adsorption paths resulting in the products of PO are competing with each other because of their comparable activation barriers (9, 8 and 9 kcal/mol,

Table 2 Comparison of activation barriers for propylene epoxidation reactions on silver oxide (001) surface and silver (111) surface (values are in units of kcal/mol)

Reactions	Ag_2O (001) surface	Ag (111) surface	
	This study[a]	Fellah [19][b]	Torres et al. [7][c]
Propylene adsorption (first C activation, propylenoxy1, step 1a)	8	14	14
Propylene adsorption (second C activation, propylenoxy2, step 1b)	9	7	–
Propylene adsorption (Π-allyl formation, step 1c)	9	6	7
Propylene oxide formation (following C1 activation, step 2b)	17	16	14
Propylene oxide formation (following C2 activation, step 3b)	20	22	–
Propanal formation (step 2c)	42	16	13
Acetone formation (step 3c)	39	36	–
Desorption of the products (step 4)			
Propylene oxide	19[d], 15[e]	–	–
Propanal	18	–	–
Acetone	18	–	–

[a] Gaussian'03/DFT/B3LYP, $Ag_{14}O_9$ (001) surface cluster

[b] Gaussian'03/DFT/B3LYP, Ag_{13} (111) surface cluster

[c] VASP/PW91, Silver oxide (001) periodic slab, CI-NEB

[d] PO was formed by step 2b

[e] PO was formed by step 3b

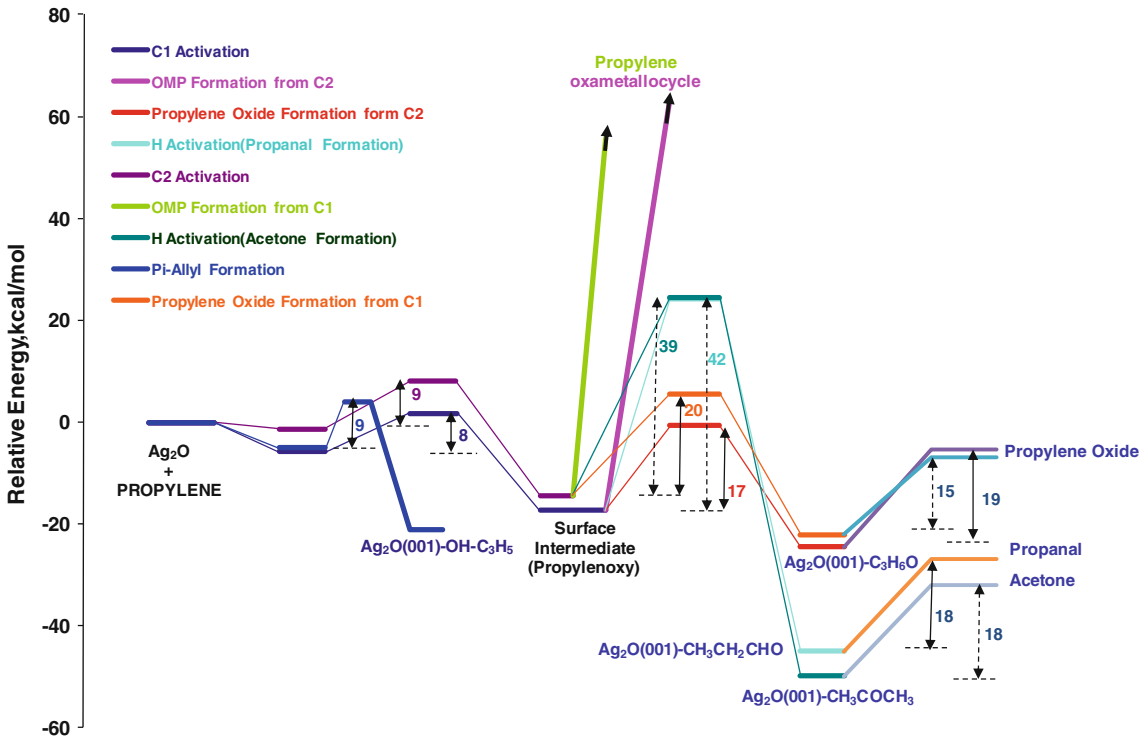

Fig. 9 A summary energy diagram showing a comparison of all the paths for propylene oxidation on (001) silver oxide surface cluster

respectively) while Π-allyl formation path is more favorable on Ag (111) surface. The propylene oxometallocycles are not probable intermediates on the Ag_2O (001) surface while these are formed on Ag (111) surface [7, 19]. According to calculations based on SO_2 adsorption, the essential reason for not obtaining oxometallocycle as an intermediate molecule on silver oxide and competition of PO and Π-allyl formation paths is lower basicity of surface oxygen atom of silver oxide compared to O atom on silver. Theoretical calculations also indicated that a surface

oxygen atom of silver oxide (001) has a higher spin density when compared to oxygen atom adsorbed on Ag (111) surface. The activation barriers (17 and 20 kcal/mol for PO formation and 39 and 42 kcal/mol for acetone and propanal formation, respectively) show that acetone and propanal have very low probabilities to be formed on Ag_2O surface while propylene oxide can be more easily formed on the cluster.

Acknowledgments The numerical calculations reported in this paper were performed at TUBITAK ULAKBIM, High Performance and Grid Computing Center (TR-Grid e-Infrastructure). This study was also partially supported by CENG HPC System of METU. We would like to thank the Scientific and Technical Research Council of Turkey (TUBITAK Project No:108T378) for financial support.

References

1. Nijhuis TA, Makkee M, Moulijn JA, Weckhuysen BA (2006) Ind Eng Chem Res 45:3447
2. Verykios XEFP, Stein R, Coughlin W (1980) Catal Rev Sci Eng 22:197
3. Sachtler WM, Backx HC, van Santen RA (1981) Catal Rev Sci Eng 23:127
4. van Santen RA, Kuipers HPCE (1987) Adv Catal 35:265
5. Grant RB, Lambert RM (1985) J Catal 92:364
6. Kizilkaya AC, Fellah MF, Onal I (2010) Chem Phys Lett 487:183
7. Torres D, Lopez N, Illas F, Lambert RM (2007) Angew Chem Int Ed 46:2055
8. Bcquet ML, Michaelides A, Loffreda D, Sautet P, Alavi A, King DA (2003) J Am Chem Soc 125:5620
9. Bocquet ML, Sautet P, Cerda J, Carlisle CI, Webb MJ, King DA (2003) J Am Chem Soc 125:3119
10. Bocquet ML, Loffreda D (2005) J Am Chem Soc 127:17207
11. Gao W, Zhao M, Jiang Q (2007) J Phys Chem C 111:4042
12. Michaelides A, Reuter K, Scheffler M (2005) J Vac Sci Tech 23:1487
13. Schmid M, Reicho A, Stierle A, Costina I, Klikovits J, Kostelnik P, Dubay O, Kresse G, Gustafson J, Lundgren E, Andersen JN, Dosch H, Varga P (2006) Phys Rev Let 96:146102-1
14. Carlisle CI, King DA, Bocquet ML, Cerda J, Sautet P (2000) Phys Rev Lett 84:3899
15. Michaelides A, Bocquet ML, Sautet P, Alavi A, King DA (2003) Chem Phys Lett 367:344
16. Bukhtiyarov VI, Havecker M, Kaichev VV, Gericke AK, Mayer RW, Schlögl R (2003) Phys Rev B 67:235422
17. Fellah MF, van Santen RA, Onal I (2011) Catal Lett 141:762
18. Ozbek MO, Onal I, van Santen RA (2011) ChemCatChem 3:150
19. Fellah MF (2009) A density functional theory study of catalytic epoxidation of ethylene and propylene. PhD thesis, Middle East Technical University, Ankara
20. Lu J, Luo M, Li HL (2002) Appl Catal A 237:11
21. Kohn W, Sham LJ (1965) Phys Rev 140:A1133
22. Frisch MJ, Trucks GW, Schlegel HB, Scuseria GE, Robb MA, Cheeseman JR, Montgomery JA Jr, Vreven T, Kudin KN, Burant JC, Millam JM, Iyengar SS, Tomasi J, Barone V, Mennucci B, Cossi M, Scalmani G, Rega N, Petersson GA, Nakatsuji H, Hada M, Ehara M, Toyota K, Fukuda R, Hasegawa J, Ishida M, Nakajima T, Honda Y, Kitao O, Nakai H, Klene M, Li X, Knox JE, Hratchian HP, Cross JB, Bakken V, Adamo C, Jaramillo J, Gomperts R, Stratmann RE, Yazyev O, Austin AJ, Cammi R, Pomelli C, Ochterski JW, Ayala PY, Morokuma K, Voth GA, Salvador P, Dannenberg JJ, Zakrzewski VG, Dapprich S, Daniels AD, Strain MC, Farkas O, Malick DK, Rabuck AD, Raghavachari K, Foresman JB, Ortiz JV, Cui Q, Baboul AG, Clifford S, Cioslowski J, Stefanov BB, Liu G, Liashenko A, Piskorz P, Komaromi I, Martin RL, Fox DJ, Keith T, Al-Laham MA, Peng CY, Nanayakkara A, Challacombe M, Gill PMW, Johnson B, Chen W, Wong MW, Gonzalez C, Pople JA (2004) Gaussian 03. Gaussian Inc., Wallingford
23. Becke AD (1988) Phys Rev A 38:3098
24. Becke AD, Roussel MR (1989) Phys Rev A 39:3761
25. Lee C, Yang W, Parr RG (1988) Phys Rev B 37:785
26. Baker J, Muir M, Andzelm J, Scheiner A (1996) ACS Symp Ser 629:342
27. Karakaya I, Thompson WT (1992) J Phase Equilib 13:137
28. Sanz-Navarro SV, Astrand PO, Chen D, Rønning M, van Duin ACT, Jacop T, Goddard WA III (2008) J Phys Chem A 112:1392
29. Mulliken RS (1955) J Chem Phys 23:1833
30. Glendening ED, Reed AE, Carpenter JE, Weinhold F. NBO, version 3.1, Theoretical Chemistry Institute, University of Wisconsin, Madison
31. Fellah MF (2011) J Phys Chem C 115:1940
32. Fellah MF, van Santen RA, Onal I (2009) J Phys Chem C 113:15307
33. Fellah MF, Onal I (2010) J Phys Chem C 114:3042
34. Fellah MF, Onal I, van Santen RA (2010) J Phys Chem C 114:12580
35. Fellah MF, Pidko EA, van Santen RA, Onal I (2011) J Phys Chem C 115:9668
36. Fellah MF, Onal I (2011) Catal Today 171:52
37. Fellah MF (2011) J Catal 282:191
38. Zhao YX, Wu XN, Ma JB, He SG, Ding XL (2011) Phys Chem Chem Phys 13:1925
39. Wu XN, Zhao YX, Xue W, Wang ZC, He SG, Ding XL (2010) Phys Chem Chem Phys 12:3984
40. Schwarz H (2011) Angew Chem Int Ed 50:10096